Pre-compliance Specific Absorption Rate (SAR) evaluation of a smart phone using Near-field Over The Air (OTA) measurements and advanced post-processing Link approach

Shoaib Anwar, Member, AMTA
Aurelien Lelievre, Member, AMTA
Nicolas Gross, Member, AMTA
MVG Industries, Villejust, France
shoaib.anwar@mvg-world.com

Francesco Saccardi, Fellow, AMTA
Lars Jacob Foged, Fellow, AMTA
Microwave Vision Italy SRL, Via dei Castelli Romani 59, 00071, Pomezia, Italy
francesco.saccardi@mvg-world.com

***Abstract*— The need for fast and accurate measurement techniques for electromagnetic exposure from modern communication devices has increased since few years. The exposure metric for frequencies up to 10 GHz is the Specific Absorption Rate (SAR). The Link approach has been studied and validated since few years to evaluate the SAR for passive antennas and some active devices which can be controlled in terms of output power and have no automatic power adjustment mechanism. In this paper, we go a step further and apply the Link approach to measure the SAR for a commercial smart phone, where we have no a priori knowledge or control, over the power control mechanism, and the antenna position inside the phone. The measurements are done with a 10MHz bandwidth LTE signal communication, between a commercial smart phone, and the Radio Communication Tester (RCT) emulating a mobile Base Station. The E-field distribution and SAR values, computed from the Link approach, are compared to results from the same DUT measured with a legacy SAR (single probe with a robot and phantom) measurement system. The results show SAR values, within 2.8% (0.1dB) for 10g SAR, and -7.1% (-0.3dB) for 1g SAR (at 5mm separation between phone and phantom), between the Link and Legacy approach. The SAR values at 0mm separation distance are calculated using extrapolation, and the difference is 7.0% (0.3dB) for 10g SAR and -6.2% (0.28dB) for 1g SAR. Based on these results, it is shown that the Link approach is a faster alternative SAR measurement approach, applicable for pre-compliance, during early stage of development, and for post-production scenarios.**

I. INTRODUCTION

Non-invasive Fast SAR techniques have garnered significant interest since the introduction of 4G. Traditional systems, such as those described in [1], involve a single E-field scalar probe sequentially scanning a liquid within a phantom to determine the maximum E-Field and subsequently the SAR around this hot-spot, which is time-consuming.

To expedite measurement time, fast SAR techniques were developed, utilizing multiple probes with a wide-band liquid phantom to conduct parallel measurements on a specific plane within the phantom. By integrating smart grid techniques and post-processing, the SAR evaluation time was significantly reduced [2],[3]. With the advent of 5G, Wi-Fi 7, and MiMO technology, alongside the coexistence of legacy technologies, SAR evaluation has become a more complex and lengthy process. Modern high-end smartphones now support over sixty frequency bands including a multitude of technologies such as: 2G, 3G, LTE, 5G FR1, 5G FR2, Wi-Fi, Bluetooth, GPS, and recently satellite link frequencies for Non-Terrestrial Network (NTN). For each frequency band, and its corresponding modulation, SAR is assessed for 1g and 10g tissue volumes across various use cases and positions (head, trunk), device orientations (left, right, front, back, tilted), with different antennas activated separately, or a combination of antennas operating with same technology (MiMo), or different technologies (power sharing). Existing single probe SAR methods can take weeks and months of measurements for a single device. The latest standard procedures accommodate both fast and traditional SAR techniques [4].

Since few years, the combination of fast Near-field measurements and simulations (or Link) approach has been applied to evaluate the SAR and power density. This method has been validated for several passive radiating elements such as, sleeve dipoles [5], standard SAR dipoles [6], quad ridge horns [7]. The results show close agreement between full wave simulations, legacy SAR measurement system, and Link Approach. In addition, this method has been applied to evaluate the quality-of-service evaluation, diagnostics, antenna placement applications [8]-[12].

A similar technique has also been applied to active devices using OTA measurements. SAR from and indoor small cell base station [13] has been evaluated using a single probe near-field measurement system, and then computing the equivalent source (Huygens's Box) using the inverse problem application. This Huygens's box is then exported to a full-wave electromagnetic solver, and a 3D model of a phantom is

introduced in simulations. To improve the interaction between the device and the phantom in the simulations, a PEC volume is inserted inside the Huygen's box. Comparing the results, with legacy single probe SAR system measurements, show a peak SAR of about 3dB lower using the Link (or OTA) approach, and 2 dB lower for 10g SAR value, at 5mm separation distance.

In [14], a Golden wireless device, mimicking a modern smart phone, with known antenna pattern, antenna position, and control over the power stability has been studied. The 10g SAR results, at 6.2 mm separation distance from Link approach, are about 0.68 dB lower than the Reference measurement (Legacy SAR bench).

In this study, we take a step further, applying the link approach to a commercial smart phone, where we do not have a priori knowledge of the antenna pattern, its position, choice between different antennas present on a smart phone for the same technology, and no output power control using the proximity sensor. Full-wave simulations are not possible for such devices without knowledge of detailed CAD model and material properties over the whole RF spectrum. The Link approach has been improved from previous works, with the aim to have better estimation of the interaction between the reconstructed Huygens's box and the phantom in the electromagnetic solver.

This study case can be of interest in different scenarios. For example, during the advanced stages of R&D and prototyping phase, where this approach can help optimize the quality of service (Radiated power, throughput) and Safety requirements (SAR & power density) in parallel without doing lengthy measurement campaigns. The Link approach can also be applied to pre-production, pre-compliance testing. And finally, also for post-production verifications to track issues in production line.

The paper is organized as follows. In section II, the device under test is presented, the reference measurement system and the Link approach procedure is described. Section III includes the test results and comparison between the three approaches. Conclusions are drawn in section IV.

II. DUT, SAR REFERENCE, AND LINK MEASUREMENT PROCEDURE, DESCRIPTIONS

A. *DUT : Commercial smart phone*

A commercial smart phone is selected for this study. In order to avoid copyright issues and conflict of interest, the information about the make and model of the phone is not disclosed. In terms of capabilities of the smart phone, it has all the functionalities representing a modern smart phone available today in the market covering all the technologies cited in the section I. The SAR evaluation has been done for different LTE frequency bands with 10 MHz bandwidth signal. Results form band#3 at 1747.5 MHz Uplink (UL) centre frequency will be presented here. The same device is measured on the legacy single probe SAR measurement system and in the near-field multi-probe measurement system. For any device to pass the FCC SAR certification, the maximum SAR limits for 1g of tissue is 1.6 W/Kg, and for 10g of tissue volume it is 4 W/Kg.

B. *Reference SAR measurements: MVG ComoSAR*

The reference SAR measurements are done using the MVG ComoSAR system. The complete details can be found in [1]. The system (shown in Figure 1) consists of a scalar isotropic E-field measurement probe mounted on a robotic arm. The DUT is placed under a liquid filled phantom emulating the RF characteristics for the measurement frequency. A Radio communication Tester (RCT) is used to emulate the LTE protocol with the required central frequency, modulation scheme, channel bandwidth, and impose maximum power transfer on the DUT.

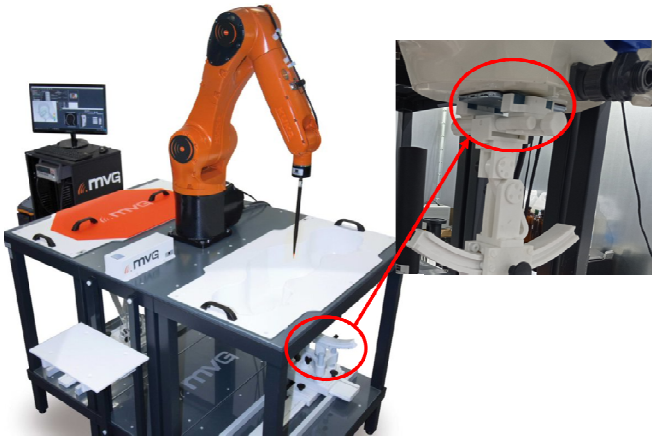

(a)

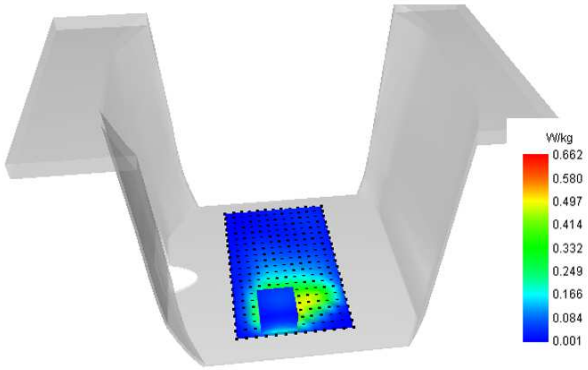

(b)

Figure 1. (a) Reference SAR measurement system with DUT, (b) SAR measured at 1747.5 MHz with 5mm seperation.

Precision spacers are used to set the DUT separation distance with the phantom skin. The MVG OpenSAR software is used to control the instrumentation, (RCT, voltage meter) robot movement, data acquisition and SAR evaluation. For this study we used a single orientation of the phone with the phone screen facing the phantom and different separation distances for the reference measurements (0, 2, 3, 4, 5, 6.2, 9.82, & 11.2 mm). LTE frequency band #3 was emulated between RCT and DUT with UL central frequency set to 1747.5 MHz and DL central frequency set to 1842.5 MHz. The channel bandwidth is 10 MHz. QPSK modulation scheme is used.

The liquid and phantom characteristics are summarized in Table I. These values are target values form the IEC / IEEE SAR standard [4]. For the measurements and simulations, we used measured tissue liquid values which are within ±10% of the target values.

TABLE I. SAR LIQUID AND PHANTOM CARACTERISTICS @1747.5 MHZ

Liquid (X xY x Z)	300 x 300 x 150 mm
Phantom (X xY x Z)	300 x 300 x 2 mm
ε_r (Phantom)	3.5
ε_r (SAR liquid)	40
Concductivity (SAR liquid)	1.4 [S/m]
Density (SAR liquid)	1000 [kg/m^3]

C. *Link measurement and post-processing*

The Link procedure is similar as stated in previous work for the Golden device [14] and is presented in Figure 2. The near-field (NF) data is measured using multi-probe near-filed MVG StarLab OTA measurement system [15] with a commercial RCT. The NF data is then imported inside the MVG Insight software [16] along with spatial representation of the DUT in the form of a closed parallelopiped shape. The equivalent currents are then computed over this closed shape representing the DUT using the Insight computation engine. It is important to recall here that that reconstruction geometry is at least one mesh-step larger than the real DUT size (at least lambda/20) in order to obtain good accuracy. This means that the SAR evaluation for 0mm separation between DUT and phantom cannot be obtained using the Link approach. The current SAR standard [4] or FCC requires the DUT to be measured, at 5mm distance for body-worn or hotspot configurations, and at 0mm separation distance for Head configuration.

To remedy this limitation, we have shown in previous works that the extrapolation from the trend curve of SAR at different distances seems to correlate well with measured data.

Once we have the Huygens's box from Insight computation, we can import this Huygens's box to any commercial full-wave electromagnetic solver and introduce the 3D model of the liquid phantom with SAR liquid. The full-wave simulation is done using CST software [17] in this study and the phantom parameters are the same as defined in the previous section. The power of the Huygens's box source, once imported in the full wave solver from Insight, is the same as obtained from the Near-filed measurements after application of the gain calibration, representing the total radiated power of the device under test.

The next step is to add the phantom model in proximity of the Huygens's box in the full wave solver at a given separation distance (one of the values from section II-B). In order to better estimate the coupling and reflections between the smart phone and the phantom, it has been reported in [13] to include a PEC volume representing the DUT size inside the Huygens's box. In this study, we go a step further to improve the model by introducing more details in the model (as done previously in [14]).

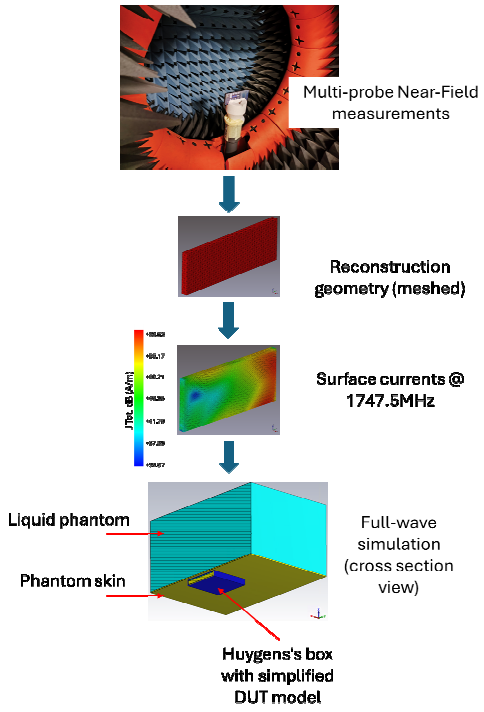

Figure 2. Work flow for Link approach applied to SAR evaluation for the smart phone.

The smart phone is modelled as a two layer structure consisting of an aluminium base (representing the phone body and the electronic components), and a glass sheet representing the screen of the smart phone. The permittivity and loss tangent of the glass sheet used in the simulation are 6.97 and 0.014 respectively. This level of detail can be obtained for a commercial smart phone from data available to public [18], and it can improve the SAR estimation as it will be shown in the next section. The thickness of the glass is estimated to be 0.8mm. It was observed that if we consider all metal PEC inside the Huygens's box, the error increases w.r.t the reference values.

III. MEASUREMENT RESULTS : LINK VS. LEGACY SAR APPROACH

The commercial smart phone was measured by the legacy SAR measurement system according to the procedure described in section II-B. 1g and 10g SAR values were computed and used as reference values to be compared with the Link approach results. The measurements were done at different separations distances as specified in section II-B, using precision spacers for the legacy system.

The results for 1g and 10g SAR are presented in Figure 3. Excellent correlation is observed between the reference measurements and the Link approach. The Link measurements are almost all withing ±10% of the reference measurements. Only the 1g SAR at 9.82mm and 11.2mm separation distance, and 10g SAR at 2mm distance, have difference of 11.7%,

11.2%, and 11.3%. It is important to note here that the SAR values from Link approach at 0mm separation are extrapolated from the measurement data at other distances. A second order polynomial trend curve is used for the extrapolation value.

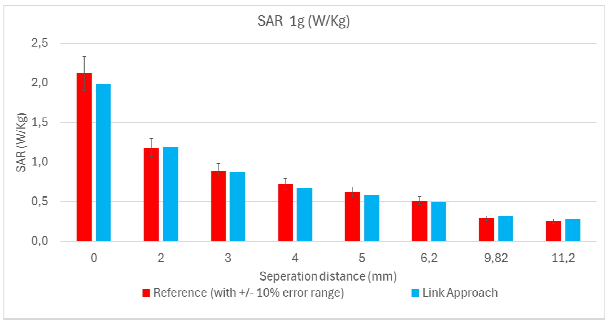

(a)

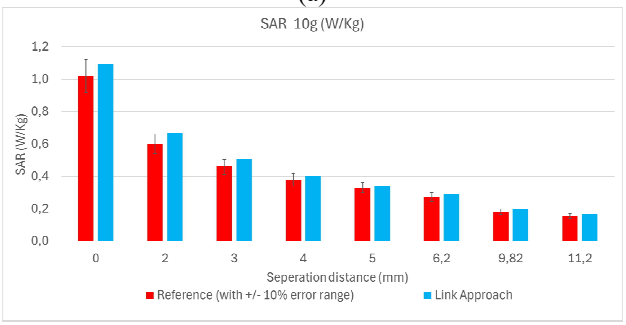

(b)

Figure 3. Measured SAR results for a commercial smart phone at different separation distances for (a) 1g, and (b) 10g volumes. Link approach values at 0mm separation are extrapolated.

In addition to the SAR values shown above, the reconstructed E-field from Link approach is also compared with the reference measurement data in Figure 4. The separation distance of 5mm is selected for comparison, as this is the one used for majority of the cases in the standard SAR reports. The plots (obtained at same position inside the phantom liquid) show a good comparison of the E-field distribution from both methods and the maximum value is very close to each other, 21.21 V/m from legacy SAR system and 21.41 V/m from the Link approach. Same scales are used for the field distribution plots. The portion of the maximum location of E-field coincides with the antenna location known for this smart phone. This is important to verify, because in modern smart phones, there are multiple antennas used for diversity gain, and MIMO configurations, to enhance the quality of service. In this study, there was no control available to select / maintain a particular antenna connection during the measurements. For Test Labs or device manufacturers who have this control, this check would not be necessary to validate the measurement results. The minor differences observed between the E-field / SAR results, from both techniques, can be attributed to, errors of positioning of the phone w.r.t the phantom in Legacy approach, and errors of positioning for reconstructed geometry from the near-field approach. In addition, the simplification of the DUT model in Link approach also contributes to these differences.

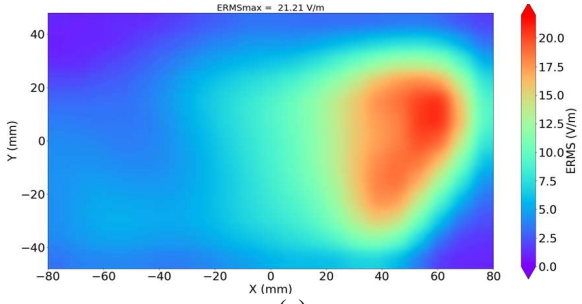

(a)

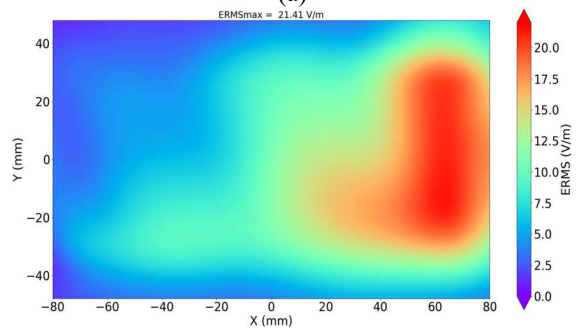

(b)

Figure 4. E-field results at 5mm separation distance between DUT and phantom for a commercial smart phone from (a) Legacy SAR, and (b) Link approach.

IV. CONCLUSION

Following on previous contributions for validation of Link approach for SAR measurements, this paper goes a step further in evaluating the 1g and 10g SAR of the commercial smart phone. The major challenge here is that we do not have any control over the antenna selection and smart power control mechanism of the device. The same phone is measured using the legacy single probe SAR system and results are compared with Link approach for a 10 MHz LTE signal, in Band 3. The SAR results, at different separation distances between the DUT and phantom, are in excellent agreement between the two approaches, with differences varying between -7.1% (-0.32dB) up to +11.7% (0.48dB) for both 1g and 10 SAR values for separation distances ranging from 0mm up to 11.2mm. The E-field distribution confirms that the same antenna is active, and the maximum values are in agreement. The Link approach provides a much faster alternative, where the measurement is done only once, without the phantom. All the separation distances, and phone orientations can be simulated in post-processing. This approach, thus presents a fast alternative to evaluate the SAR for modern communication devices, which have multiple technologies integrated and measurement time is directly proportional to, the number of frequencies, times the number of orientations, times the number of separation distances, times the number of connection parameters. Using the Link approach, we can reduce the measurement time by the order of two factors (orientations & separation distance). This is a considerable improvement, specially in, advanced R&D phase, pre-compliance phase, and post-production phase (recycled / refurbished devices) of the device life cycle.

REFERENCES

[1] MVG ComoSAR V5 measurement system, https://www.mvg-world.com/fr/produits/sar/sar-systems/comosar-v5.

[2] R. Butet *et al*., "Easy to use real time SAR measurements system," *2013 7th European Conference on Antennas and Propagation (EuCAP)*, 2013, pp. 1559-1560.

[3] ART-MAN SAR system from Art-Fi, 2013, https://www.art-fi.eu/art-fi/about-art-fi/about-art-fi2020.

[4] IEC/IEEE 62209-1528:2020, "Measurement procedure for the assessment of specific absorption rate of human exposure to radio frequency fields from hand-held and body-worn wireless communication devices - Human models, instrumentation and procedures (Frequency range of 4 MHz to 10 GHz)", published 19th October, 2021.

[5] L. Scialacqua, S. Anwar, J. F. Mioc, J. Luc, A. Lelievre, M. Mantash, N. Gross, L.J. Foged, "Experimental Validation of Non-Invasive SAR Evaluation from Measurements and Numerically Assisted Post Processing", *2022 Antenna Measurement Techniques Association Symposium (AMTA)*, 2022.

[6] S. Anwar, L. Scialacqua, A. Lelievre, M. Mantash, J. Luc, N. Gross, F. Saccardi, L. J. Foged, "Advanced Post-Processing Technique to Evaluate Specific Absorption Rate (SAR) for a Standard Dipole Antenna," *2024 18th European Conference on Antennas and Propagation (EuCAP)*, Glasgow, United Kingdom, 2024, pp. 1-4,

[7] F. Mioc, L. Scialacqua, A. Scannavini, S. Anwar and L. J. Foged, "Power Density Evaluation of Simulated and Measured Data Based on Equivalent Currents Method," *2021 15th European Conference on Antennas and Propagation (EuCAP)*, 2021, pp. 1-4, doi: 10.23919/EuCAP51087.2021.9411062.

[8] J. L. Araque Quijano, G. Vecchi, "Improved accuracy source reconstruction on arbitrary 3-D surfaces," Antennas and Wireless Propagation Letters, IEEE, 8:1046–1049, 2009.

[9] J. L. A. Quijano, G. Vecchi, L. Li, M. Sabbadini, L. Scialacqua, B. Bencivenga, F. Mioc, L. J. Foged, "3D spatial filtering applications in spherical near field antenna measurements," AMTA 2010 Symposium, October, Atlanta, Georgia, USA.

[10] L J. Foged, L. Scialacqua, F. Saccardi, F. Mioc, "Measured Antenna Representation of Flush Mounted Antennas for Computational Electromagnetic Solvers," 10th European Conference on Antennas and Propagation, EuCAP, April 2016, Davos, Switzerland

[11] G. L. J. Foged, L. Scialacqua, F. Saccardi, F. Mioc, G. Vecchi. J. L. Araque Quijano, "Antenna Placement based on Accurate Measured Source Representation and Numerical Tools," IEEE Antennas and Propagation Society International Symposium, July 19-24, 2015.

[12] L. J. Foged, L. Scialacqua, F. Saccardi, F. Mioc, D. Tallini, E. Leroux, U. Becker, J. L. Araque Quijano, G. Vecchi, "Bringing Numerical Simulation and Antenna Measurements Together," IEEE Antennas and Propagation Society International Symposium, July 6-11, 2014.

[13] B. Derat *et al*., "Base Station Specific Absorption Rate Assessment Based on a Combination of Over- The-Air Measurements and Full-Wave Electromagnetic Simulations," *2021 Antenna Measurement Techniques Association Symposium (AMTA)*, 2021, pp. 1-6, doi: 10.23919/AMTA52830.2021.9620622.

[14] L. Scialacqua, S. Anwar, J. F. Mioc, A. Lelievre, M. Mantash, J. Luc, N. Gross, L.J. Foged, "Non-Invasive SAR Using OTA Measurements and Numerical Post Processing," *2023 17th European Conference on Antennas and Propagation (EuCAP)*, Florence, Italy, 2023, pp. 1-5.

[15] https://www.mvg-world.com/en/products/antenna-measurement/multi-probe-systems/starlab, MVG StarLab datasheet.

[16] https://www.mvg-world.com, INSIGHT softwave, Microwave Vision Group (MVG).

[17] https://www.3ds.com, CST STUDIO SUITE, Dassault Systems.

[18] Gorilla Glass specifications, https://www.corning.com/microsites/csm/gorillaglass/PI_Sheets/2020/Corning%20Gorilla%20Glass%205_PI%20Sheet.pdf.